Dynamic polymer hydrogels as synthetic extracellular matrices for 3D cell culture

Liu, T.

CHAPTER 1

Introduction

1.1 Cell culture models for *in vitro* drug screening

The failure of therapeutics in late-stage clinical trials is largely due to drug safety issues in addition to therapeutic insufficiency. A database of phase II and phase III clinical trials over the past 7 years shows that more than half of all drugs (52%) fail due to insufficient efficacy, and about 24% of drugs fail in phase II due to safety issues including a low therapeutic index.[1] The low drug success rate and high costs during drug discovery pipeline poses an urgent need for researchers to develop new strategies for early and precise prediction of drug therapeutic effect and safety issues.

In vitro cell culture models have become valuable tools to examine drug effectiveness and screening drug toxicity as an intermediate step prior to animal and human clinical trials because of their use of accessible cell sources and scalability. Cells used in these screens are isolated from their native environment and cultured on rigid plastic surfaces in 2D *in vitro*, in a monolayer with limited cell-cell contacts. Though this culture setup is routinely used, cells cultured as a monolayer often exhibit different drug reactivity and sensitivity in comparison to their growth *in vivo*.[2] When cultured on 2D surfaces, some native tissue-derived primary cells (*e.g.* primary hepatocytes) may rapidly lose their functional properties or differentiate.[3] This behavior is unsurprising as cells cultured on 2D surfaces lack the complexity of *in vivo* tissues that provide a three dimensional (3D) structural environment, cell-cell contacts, oxygen and nutrition gradients, as well as multiple cell types. One solution to overcome this challenge is to use multicellular models where the cells are aggregated in compact structures in 3D providing cell-cell contacts, a hypoxic environment, as well as oxygen and nutrient gradients.[4] Spheroids composed of hepatocellular carcinoma cells (HepG2) displayed higher expression (such as CYP2C9, CYP3A4, ALB, UGT1A1) of hepatocyte-related genes when cultured as spheroids in agarose microwells showing increased resistance against antitumor agents in comparison to their culture as a monolayer.[5] Breast cancer cells (MDA-MB-231) assembled into 3D tumor spheroids

within collagen hydrogels were reported to show more robust chemosensitivity during drug treatment in comparison to their culture in 2D.[6] Moreover, Burdick and co-workers recently developed heterogeneous spheroids based on cardiomyocytes and cardiac fibroblasts and demonstrated their use as effective models for engineering scarred cardiac microtissues and their application for therapeutic screening of mRNAs.[7] These examples highlight that moving from 2D to 3D spheroid culture is an efficient means to narrow the gap between *in vitro* and *in vivo* conditions.

1.2 Developing 3D cell culture models *in vitro*

The assembly of cells into 3D structures can involve either scaffold-free or matrix-based (*e.g.* hydrogels) approaches (Figure 1.1). In scaffold-free culture, cell spheroids form 3D structures due to aggregation in a hanging drop, on non-adhesive surfaces or through agitation by continuous stirring. By seeding cells into 96-well ultra-low attachment plates, the Eccles group has developed a 3D spheroid culture protocol for 40 tumor cell lines.[8] The spheroid sizes of different cell lines are maintained in a range of 300-500 μm by optimizing initial cell seeding densities. Within this study, the tightly compacted U-87 MG spheroids show tumor hypoxia transporters and rapid invasion into Matrigel, which indicating cell movement and matrix degradation occur. While 3D spheroids were produced from several cell lines besides U-87 MG, the technique usually involves considerable efforts to optimize culture conditions and special equipment can be required (*i.e.* to agitate the culture). In contrast, matrix-based 3D cell culture involves the use of materials based on hydrogels that can be from natural or synthetic sources to provide a water-rich environment with cues that stimulate cells biophysically or biochemically. More specifically, features of such matrices that have been tuned include cell-adhesiveness through peptide or protein cues, stiffening, micro/macro structure, hydrophobicity and porosity, opening the door to developing *in vitro* cell culture models for a broad range of biological applications.

Besides the increased microenvironmental complexity by moving from 2D to 3D culture, the wide availability of various cell sources provide a platform for researchers to develop increasingly complex *in vitro* cell culture models to answer a broad range of *in vivo* questions in biomedical research. For the liver, a large variety of cell types have been examined to develop models to advance drug toxicity testing, drug discovery and disease modeling. Cell types such as primary human hepatocytes (PHH), hepatoma cell lines (HepG2, HepRG), and hepatocytes derived from stem cells (adult (ASCs), human embryonic (hESCs) and induced pluripotent (iPSCs) iPSC-derived)) each with their various benefits and challenges.[5] More recently, iPSCs are being examined for such applications with great interest because they can provide an inexhaustible source of hepatocytes that can be derived from a patient through reprogramming to provide a personalized view into these areas.[9]
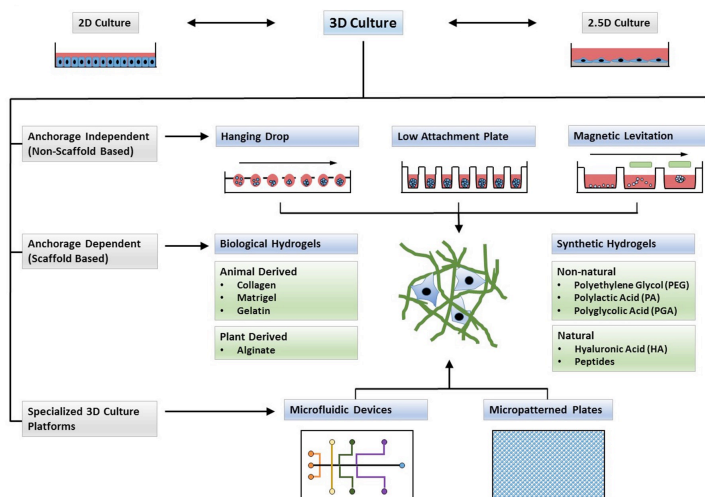

Figure 1.1. Cell culture techniques. In 2D culture, cells are cultured as a monolayer on stiff surfaces, whereas in 2.5D culture cells are plated on a thick layer of ECM-derived materials. Scaffold-free approach (3D self-assembled spheroids culture) or matrix encapsulation (natural ECM-derived materials and synthetic hydrogels) have been applied in 3D. Microfluidic devices and micro-patterned plates can also be involved to provide hybrid and complex microenvironments. Imaged adapted from reference [10].

1.3 Human induced pluripotent stem cell culture

Induced pluripotent stem cells were first reported by Yamanaka in 2006 when his group derived cells that displayed the same morphology and growth as embryonic stem cells (ESCs) by transfecting adult mouse fibroblasts with four reprogramming factors Oct3/4, Sox2, c-Myc and Klf4.[11] Soon after, human induced pluripotent stem cells (hiPSCs) were developed successfully using an optimized retroviral transduction of adult human fibroblasts, paving the way for their application in areas such as tissue engineering, cell transplantation and drug discovery unlocking the potential for a personalized approach.[12] Moreover, this class of cells is attractive for these applications due their capacity for self-renewal, potential to be differentiated to numerous cell types,[13] accessibility,[14,15] available optimized reprogramming protocols,[16–18] lack of ethical controversies in comparison to ESCs and immunocompatibility.[19–23]
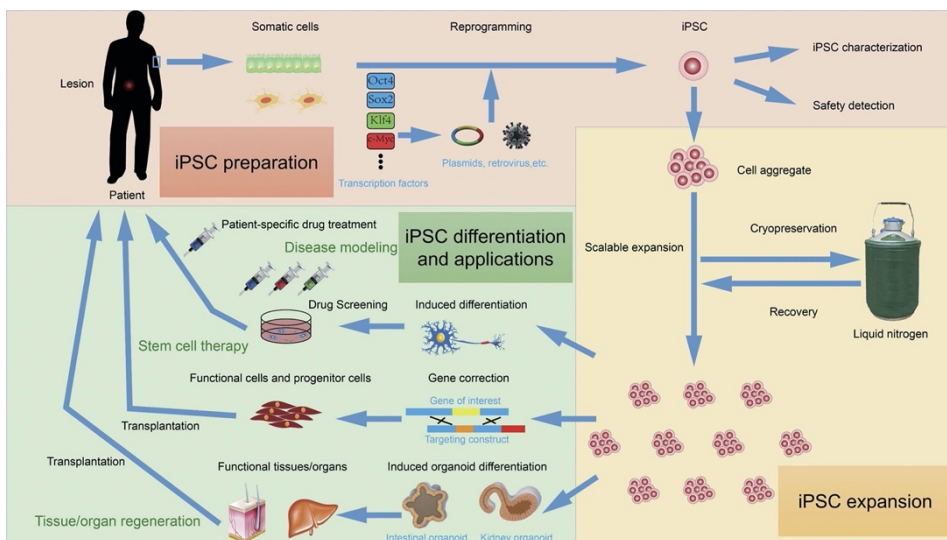

Figure 1.2. iPSCs workflow. Imaged adapted from reference [24].

Initially, 2D culture was the commonly used method to expand hiPSCs in combination with a feeder layer based on mouse embryonic fibroblasts (MEFs). This feeder layer provides growth factors, cell-binding proteins and cell-cell contacts to

support iPSC growth. However, MEF feeder layers can contaminate the stem cell culture with animal pathogens such as retroviruses because of their allogeneic nature. Optimization of a human feeder layer would decrease the immune response and remove its exposure to animal pathogens, however the undefined components and variability in the culture remain challenging.[25] As an alternative to feeder layers surface coatings based on Matrigel™, a commercially available feeder-free tumor derived ECM mixture, or recombinant proteins, such as vitronectin and laminin, have been used. Short peptides have also examined for this purpose because of their synthetically accessible character. Cell-adhesive peptides that target integrin receptors, such as RGD, have been coupled to acrylate polymer surfaces to support cell attachment, proliferation and specific differentiation of stem cells. This 2D culture scaffold is commercially sold as Synthemax™.[26,27] Moreover, Kiessling and co-workers developed a 2D substrate that displays heparin-binding peptides to interact with cell-surface glycosaminoglycans for long-term hES culture (3 months) showing high levels of pluripotency markers and maintenance of normal karyotype.[28] Although platforms for iPSC culture in 2D have advanced significantly, unsolved issues remain such as limited space for growth, diverse physiological functions in different clones, spontaneous differentiation during culture and cumbersome protocols to expand cells into the required cell quantity.

Expansion of iPSCs has been further examined in 3D to provide a more *in vivo*-like environment and space due to the added culture dimension. Matrix-free approaches in 3D have demonstrated that hiPSCs can self-assemble into spheroids, organoids or cell aggregates in liquid medium. Set-ups such as spinner flasks, rotating wall vessels and stirring bioreactors have been used with agitation to allow nutrient and gas exchange. Still challenges remain in optimizing culture conditions, including pH, temperature and dissolved oxygen concentrations, removal of metabolites, waste products and cell agglomeration can occur resulting in lower volumetric yields. Additionally, continuous

shear forces can induce cell death during iPSC culture.[29] As a consequence, gel embedding of these cellular aggregates is a offen used strategy to overcome some of these challenges. The iPSCs can be either encapsulated during the gelation process of polymer solutions, or the cells can be directly mixed with the gel depending on its mechanical properties, namely its capacity for self-recovery. In 2013, Lei *et al.* embedded hiPSCs in a thermoresponsive block co-polymer hydrogel and obtained ~20-fold expansion of hiPSCs per passage in a 5-day culture. The hiPSCs were proven to maintain a high level of pluripotency and normal karyotype after a 280-day culture with the hydrogel, that is ~10^{72} fold expansion after 60 passages.[28] However, these hydrogels are based on polymers of a high molecular weight where it would be challenging to introduce biological cues for further applications, for example, cell differentiation, highlighting the need for small molecules in a defined manner.

hiPSCs are a potent cell source for developing *in vitro* cell culture models because of their capacity to differentiate into virtually any cell type of the human body. For example, hiPSCs can give rise to cardiomyocytes (CMs), endothelial cells (ECs) or vascular cells using specific differentiation protocols, offering a platform to study and explore heart disease *in vitro* in a personalized manner starting from patient material.[30] By co-assembly of hiPSC-CMs and hiPSC-ECs, Mummery and co-workers have successfully fabricated 3D cardiac microtissues *in vitro*.[31] Moreover, differentiated cells derived from hiPSCs show great potential for cell-based therapeutic applications. For example, hiPSC-derived CMs from healthy donors have been demonstrated to support cardiac reconstruction by enhanced engraftment, cell proliferation and treatment of heart infarct.[32–34] Luo *et al.* developed a 3D approach involving nanofiber hydrogels to enhance hiPSC differentiation to hepatocytes by mimicking their *in vivo* environment. HiPSCs embedded within the hydrogel differentiated into hepatocyte-like cell spheroids and displayed higher levels of albumin secretion, urea production and glycogen synthesis compared to hiPSCs

differentiated in 2D culture.[35] One common prerequisite for these strategies to achieve the 3D culture condition is to incorporate materials, either natural or synthetic, that provide both structural and biological support for cells.

1.4 The Extracellular matrix (ECM) of stem cell niche

In their native environment *in vivo*, cells are surrounded with a hydrated and dynamic network of macromolecules, otherwise known as the extracellular matrix (ECM). The ECM is diverse in composition in between different tissues and areas of the body within with respect to its components, concentrations and structures. The ECM has a high water content being constructed from cell interactive proteins and proteoglycans (PGs). Consequently, ECM-derived proteins, such as collagens, elastins, fibronectins and laminins, have been widely explored for use as stem cell culture substrates.[36] For example, recombinant vitronectin and laminin-511 are used as defined long-term culture substrates for self-renewal and maintenance of hESCs.[37,38]

The extracellular microenvironment is comprised of bioactive cues that can be grouped into three major categories based on their origin: 1) physical signals from insoluble macromolecules (fibrillar proteins, glycoproteins and hydrophilic proteoglycans); 2) biochemical signals from soluble molecules (growth factors, chemokines and cytokines); 3) signals from cell-cell interactions. In general, the biophysical and biochemical signals are communicated from the outside-in through cell surface receptors (*e.g.* integrins) and are subsequently processed through intracellular signaling pathways, enabling cell responses such as coordinated differentiation, proliferation and migration to apoptosis and other specific cell functions (Figure 1.3).
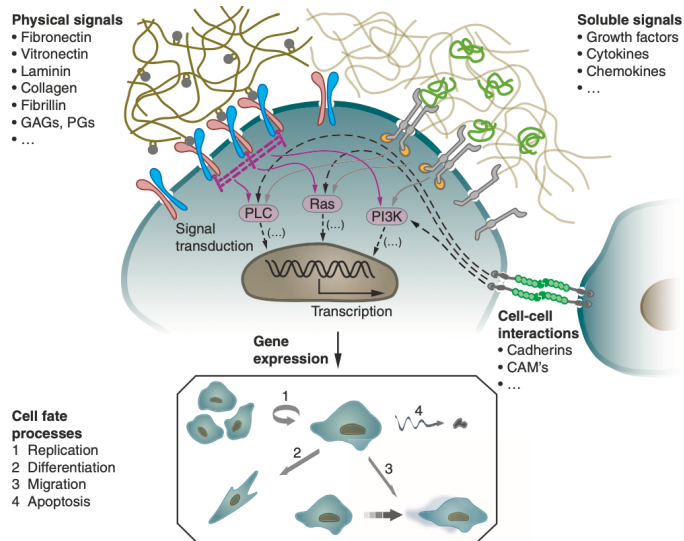
Physical signals
• Fibronectin
• Vitronectin
• Laminin
• Collagen
• Fibrillin
• GAGs, PGs
• ...

Soluble signals
• Growth factors
• Cytokines
• Chemokines
• ...

Signal transduction

PLC   Ras   PI3K
(...)   (...)   (...)

Transcription

Gene expression

Cell-cell interactions
• Cadherins
• CAM's
• ...

Cell fate processes
1 Replication
2 Differentiation
3 Migration
4 Apoptosis

Figure 1.3. Extracellular matrix: fibrous proteins and hydrated proteoglycan form a gel-like network that is composed of soluble signals (*e.g.* growth factors) and physical signals that interact through cell surface receptors (*e.g.* integrins), as well as cell-cell interactions. Image adapted from reference [39].

The microenvironment of a stem cell, also known as the "stem cell niche", consists not only the ECM components, but also supportive stromal cells, vascular tissues as well as secreted soluble factors that initiate cell-cell interaction or signaling cascades. All these factors effect stem cell behavior in concert, and vice versa, they remodel the matrix in response to signals received from their microenvironment. Stem cells can directly interact with ECM proteins through their cell surface integrin receptors, for example, integrin $\alpha v \beta 5$ mediates cell adhesion on vitronectin and integrin $\alpha 6 \beta 1$ mediates adhesion to laminin.[40] Some ECM proteins and PGs can act as a reservoir and distribute growth factors, providing them to the stem cell. On the other hand, the degradation of PGs by metalloproteinases releases growth factors that induce the remodeling of ECM microenvironment.[41,42] Moreover, the ECM shows complex dynamics in time and space that dramatically affect stem cell fate, especially during stem cell differentiation, *e.g.* in cardiac differentiation, the stiffness of the ECM

changes significantly from the embryonic (less than 500 Pa) to the adult stage (10 kPa).[43]

Several studies have demonstrated that stem cells cultured in matrices of a similar stiffness to the original tissue promote cell differentiation into the same lineage. For example, stiff substrates with an elasticity of 25-40 kPa supported differentiation of mesenchymal stem cell into bone tissue while soft substrates with an elasticity of 0.1-1 kPa were neurogenic favouring neural lineage specification. Moreover, efficient self-renewal and regeneration of skeletal muscle stem cells was observed when cells were exposed to substrates of an intermediate stiffness (12 kPa).[44–46] Because of the known role of the ECM in these processes, researchers are focusing on materials strategies that can direct and control stem cell fate through manipulation of this interface. Mooney *et al.* demonstrated that osteogenic differentiation of mesenchymal stem cells can be controlled by modulating the stiffness of the 3D microenvironment using substrates from 11 to 30 kPa. Later, by changing the elasticity of a porous hydrogel they obtained significantly improved survival, osteogenesis and bone regeneration of the transplanted stem cells in 3D.[47,48]

1.5 Synthetic covalent hydrogels as ECM mimicking materials

With the growing knowledge in the field of cell biology, researchers are developing a comprehensive chemical picture of the extracellular matrix and functions, such as its capacity to control cell fate. Rebuilding the *in vivo* cell ECM microenvironment in synthetic materials for 3D cell culture would open the door to regulate cell behaviors *in vitro*, such as cell viability, migration, proliferation and differentiation into specific cell lineages for a wide range of biomedical applications. Synthetic polymer hydrogels have been widely applied in this area. Generally, they are insoluble, crosslinked networks that contain a large quantity of water. They show several advantageous properties to mimic the their microenvironment, namely through their water-rich character,

cytocompatibility, structural and mechanical-likeness to the natural ECM.[49] Moreover, the use of specific chemistries within the materials enables precise control over their properties including structural features, mechanical stiffness, cell adhesion, and degradability, that all together play crucial roles in regulating cell morphology, migration and differentiation (Figure 1.4). Pahapale *et al.* fabricated a gelatin hydrogel platform for 3D cell culture, in which the mechanical stiffness can be controlled from soft (400 Pa) to stiff (50 kPa) with hierarchical curvature ranging from 12-120 μm to 1-4 mm (cellular length). The flexibility in tuning various materials properties makes it possible to mimic aspects of native tissues such as stiffness, as well as *in vivo* shapes and forms similarly to those found in intestinal villi, blood vessels and epithelial tissues.[50] Zhang *et al.* were able to modify gene expression profiles of neuronal cells by varying the hydrogel stiffness by increasing the $CaCl_2$ concentration of alginate/Matrigel composite hydrogels, further mimicking the properties of the brain respect to specific regions and different developmental stages.[51]
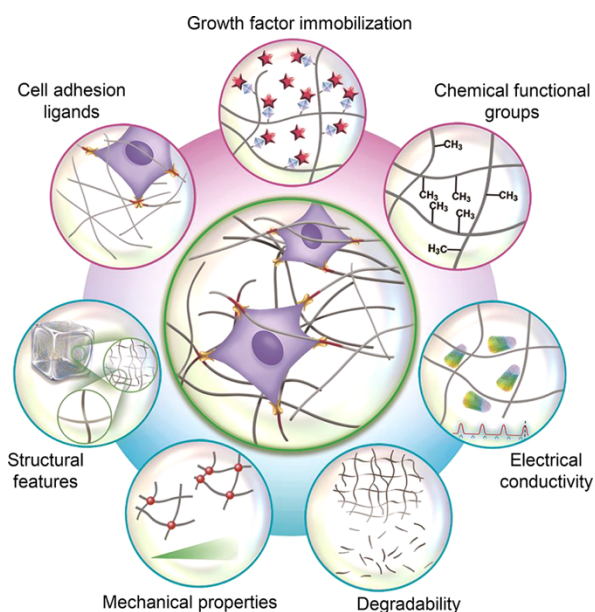

Figure 1.4. Properties of polymer materials used to recapitulate the 3D cell microenvironment. Image adapted from reference [52].

1.5.1 Modulation of mechanical cues

Hydrogels derived from natural polymers (*e.g.* collagen, Matrigel) are biocompatible, biodegradable and generally mechanically soft due to the physical nature of the interactions between their biopolymer chains. Collagen hydrogels can be prepared with shear moduli ranging from 13 to 254 Pa by adjusting the polymer concentration from 1.5 to 6 mg/mL. Though adjustable, their weak mechanical properties restrict their use to applications that require stiffnesses lower than 500 Pa. In contrast, synthetic hydrogels that are chemically defined can be outfitted with controlled cross-linking degrees and specific chemistries. Numerous cytocompatible polymers, such as the widely used poly(ethylene glycol) (PEG), the thermosensitive polymer poly(N-isopropylacrylamide) (PNIPAAm) and their derivatives, have been used as synthetic cell culture substrates. [53] Their amenability to be combined with various cross-linking chemistries, such as *in situ* radical polymerizations, mild schiff base reactions and the fast and efficient click reactions (*e.g* Diels-Alder reaction, thiol-ene addition and azide–alkyne cycloaddition) make them attractive due to their flexibility.[54] Using such cross-linking methods in combination with adjusting the monomer/polymer concentration, control over the crosslink density and thus, mechanical properties of the resultant materials can be achieved. For example, varying the monomer molecular weight, polymer concentration, ultraviolet (UV) light intensity and exposure time resulted in PEG diacrylate (PEGDA) hydrogels that show a wide range of compressive moduli from 0.7 to 233 kPa.[55] Moreover, the mechanical properties of hydrogels can be controlled spatiotemporally to further tune the cell microenvironment on-demand through a UV light-induced crosslinking strategy. Anseth's group designed a two-step crosslinking strategy in PEG hydrogels that contain SPAAC crosslinker that reacts initially without light and can be reacted further on-demand using light. Using this material, encapsulated myoblasts were observed to dynamically respond to the

changes in hydrogel stiffness in two stages by displaying increased circularity and nuclear localization of Yes-associated protein 1 (YAP) (Figure 1.5).[56]
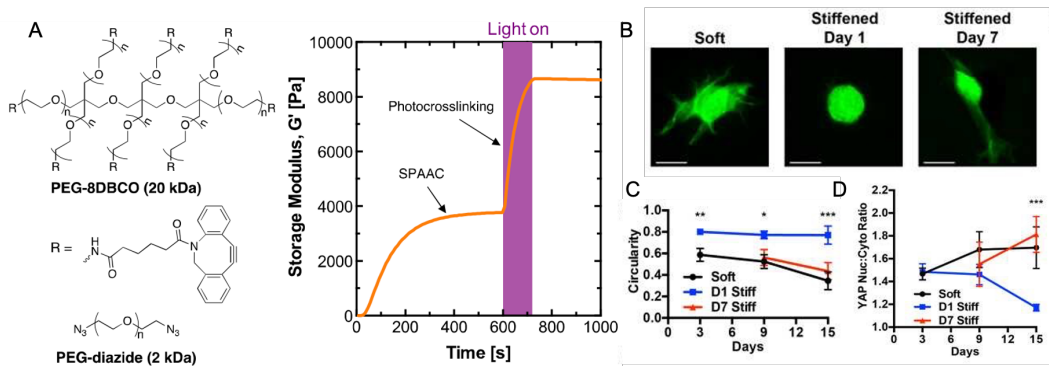

Figure 1.5. A) Primary crosslinking through azide and cyclooctyne (SPAAC) gives an initially soft hydrogel network. UV light-induced crosslinking of unreacted cyclooctyne functionalities improves hydrogel mechanical stiffness in a spatiotemporally controlled manner. B) Morphology of myoblasts cells encapsulated in SPAAC and UV light crosslinked hydrogels over a 15-day culture period. Cells were fluorescently-labelled with CellMask Green. C) Quantitative analysis of cell circularity of myoblasts cells over the 15-day culture, in which lower values indicated more spreading cells. D) Quantification of YAP nuclear over cytoplasmic localization using fluorescence intensity. Image adapted from reference [56].

1.5.2 Use of short peptides

In vivo, biological signals are transmitted via signaling molecules or proteins that are either tethered to the ECM or in solution. Hence, various synthetic peptides that are derived from ECM proteins, also called cell adhesive peptides (CAPs) have been included widely in synthetic polymer materials for cell culture applications. Besides their facile synthesis and stability during chemical processing, short sequence CAPs are the functional sequences of ECM proteins and can induce biological responses in cells. Broadly used peptide sequences include fibronectin-derived RGD, REDV and PHSRN,

YIGSR, IKVAV and PDGSR from laminin and collagen-derived DGEA.[57] Covalent attachment of these peptides into hydrogels has used reactions that involve the thiol, amino or carboxylic groups of the peptides or through their unnatural modification (*e.g.* with azides) that enable bioothogonal reactions. For example, cysteine-terminated peptides (RGD, YIGSR, PHSRN, IKVAV) can be easily coupled onto PEG polymers by the thiol–ene reaction using UV light.[58,59] The copper (I)-catalyzed alkyne azide 1,3-dipolar cycloaddition (CuAAC) click reaction is also frequently used in peptide conjugation because of its remarkable efficiency under mild conditions. The incorporation of the RGD peptide using the CuAAC reaction in a PEG-based hydrogel demonstrated improved cell attachment and enhanced cell proliferation.[60] Thus, using bioactive short peptides in combination with structurally tunable synthetic polymer matrices opens the door for user-defined control over cell growth and tissue formation for wide range application healthcare applications involving 3D cell culture.

1.5.3 Dynamic covalent bonds

Hydrogel materials used in the biomedical field largely consist static or permanent covalent bonds as they can provide a range of mechanical stiffness and stability. However, these irreversible bonds limit possibilities to recapitulate ECM dynamics that play important roles in facilitating various cell behaviors, for example, vascular morphogenesis.[61] Consequently, there is an interest in using networks based on dynamic covalent bonds, where their reversibility enables the material to form, break and reform as necessary to better mimic the ECM, but also for their practical application. Various chemistries have been used to prepare dynamic covalent hydrogels such as boronate,[62,63] disulfide,[64–66] Diels–Alder adducts,[67,68] thioesters,[69,70] Schiff-base,[71,72] or hydrazone bonds.[73–76] Using boronate-based chemistry, Anseth and co-workers designed three boronic acid variants that reacted with nitro-dopamine and formed hydrogels with different stiffnesses and relaxation

times: the strongest bond showed the longest relaxation time indicating slow dynamics and the weakest bond showed the shortest relaxation time meaning faster dynamics. Because of the rapid breaking and reforming of the hydrogel network, they were completely dissolved in the presence of cell culture media, and a second covalent crosslink was necessary to perform cell culture experiments. Human mesenchymal stem cells (hMSC) cultured in the rapidly relaxing matrix showed a more spread cell morphology, larger nuclear volume and localization of YAP/TAZ, meaning that cells engage with the dynamic matrix (Figure 1.6).[62] Similarly, a novel adaptable network was designed based on static thiol-ene photopolymerization and dynamic thiol-thioester exchange reactions. The hMSC encapsulated in these adaptable hydrogels showed reduced circularity in 3D and displayed an increase in proliferation compared to those cultured in purely static networks.[70] Moreover, Lutolf's group demonstrated that a mechanically dynamic PEG hydrogel promoted the growth of intestinal stem cells and their self-organization into organoids.[77] By introducing dynamic covalent chemistries into synthetic hydrogels, the door is open to assemble more complex tissue constructs by further mimicking *in vivo* microenvironment.
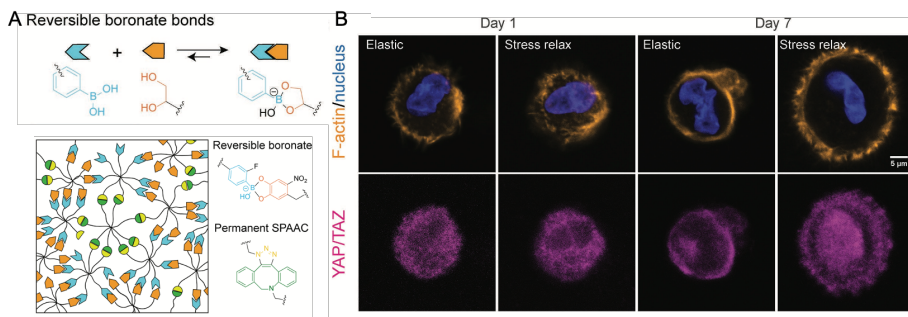
Figure 1.6. A) Two bioorthogonal crosslinking chemistries result in the formation of stress-relaxing hydrogels: dynamic bonds between boronic acids and cis-1,2-diols, and permanent and static SPAAC reactions between an azide and cyclooctyne; B) The hMSCs cultured in stress-relaxing hydrogels demonstrate a transition from YAP/TAZ in the cytosol to its nuclear localization. Image adapted from reference [62].

1.6 Supramolecular polymer materials: a new generation

Although covalent hydrogels have been frequently employed in biomaterials for *in vitro* cell culture, there remains a demand to develop materials that more closely mimic the structure and function of natural tissues with greater control over their properties. In contrast to covalent polymers, supramolecular polymers make use of monomers that are linked together through noncovalent interactions to form materials that have properties such as modularity, tunability, responsiveness and biomimicry due to the inherent dynamic nature of the bonds that hold them together. The non-covalent interactions used in their construction include highly directional hydrogen bonds, π-stacking, hydrophobic forces, ionic and host-guest interactions. In general, supramolecular materials can be prepared through one of the two approaches: 1) one-dimensional supramolecular stacking of monomers to form high aspect ratio

assemblies and 2) molecular recognition induced crosslinking of oligomeric/polymeric precursors (Figure 1.7).[78]
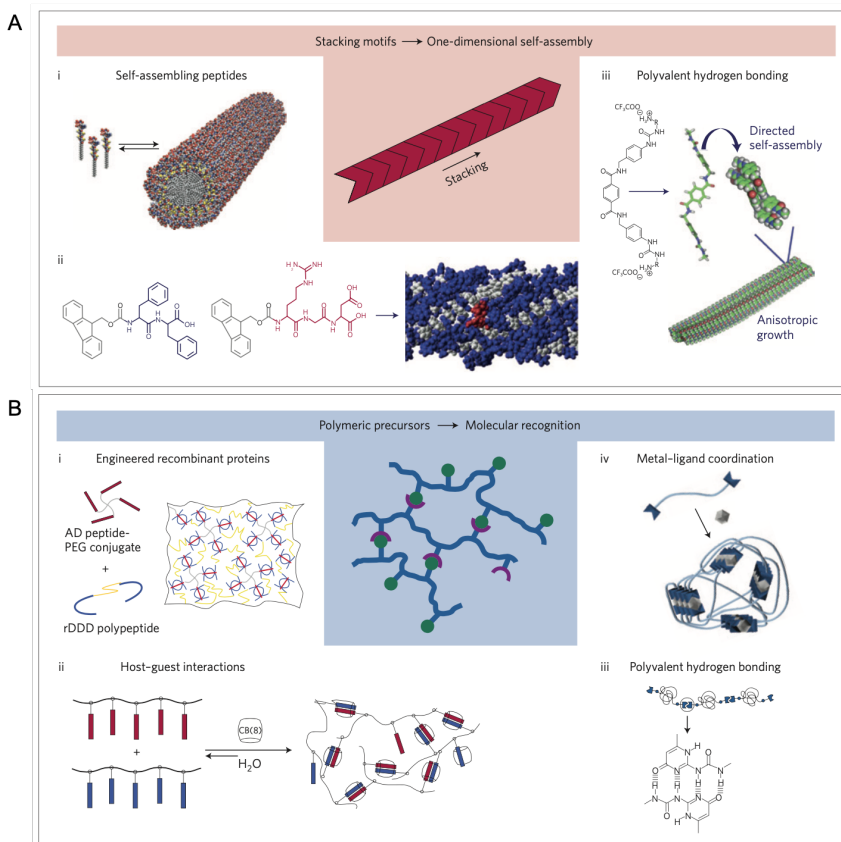
Figure 1.7. Overview and examples of supramolecular building blocks used in the construction of biomaterials. One-dimensional supramolecular stacking of monomers (top) and molecular recognition induced crosslinking of polymeric precursors (bottom). Image adapted from reference[78].

A frequently investigated class of supramolecular materials based on monomer stacking consist of self-assembling peptides. For example, the assembling peptide RADA16, also known as the commercialized product PuraMatrix, uses ionic interactions to facilitate stacking between peptides. Positively charged arginine (R) residue interact electrostatically with aspartic acid (D) and hydrophilic-hydrophobic forces between the alanine units (A), to drive the formation of β-sheets and fibrous self-assemblies with

diameters of 10 nm (Figure 1.7A). The RADA16 peptide-based matrix has shown the potential to support cell attachment and neuronal differentiation, extensive new neuronal projections as well as formation of functional junctions.[79] In an acute injury in a hamster's brain model, this peptide nanofiber scaffold enabled active neural cell migration and formation of abundant junctions, creating an environment for nerve fiber regeneration that reconnects the brain tissues together with sufficient density and function.[80] Moreover, this matrix encouraged the encapsulated stem cells to differentiate into neuronal lineages, which was further transplanted into mouse brains as a treatment demonstrating their use in direct medical application.[81,82] Another outstanding example of peptide-based assembly involves peptide amphiphiles (PAs). PAs consist of hydrophilic amino acids and a long lipophilic tail that induces β-sheet self-assembly and hydrophilic-hydrophobic interactions (Figure 1.7A). Stupp and co-workers have had a long-standing research interest in the self-assembly of PAs and their potential as functional biomaterials for tissue regeneration and cancer therapy. In 2001, the first PA with a peptide sequence of CCCCGGGS(^{PO4})RGD and a C_{16} alkyl tail was reported that yielded high aspect ratio cylindrical nanofibers under physiological conditions through intermolecular packing (Figure 1.8A).[83] Soon after, by changing the amino acid sequences and aliphatic chain length, Stupp and co-workers were able to make nanofibers with various morphologies and surface chemistries demonstrating their versatile composition and potential to fabricate various nanomaterials. Besides the use of pH changes to facilitate their self-assembly, their group also found that self-assembly of the monomers can be driven through their drying on a surface or addition of divalent cations.[84,85] Furthermore, by introducing charged amino acids at the hydrophilic region, researchers have demonstrated that charged self-assemblies can be formed that enable their binding to growth factors,[86] DNA,[87] or glycosaminoglycans,[88] broadening their use in the healthcare area. However, it still remains challenging to improve the efficiency and scale of functional peptide

monomers synthesis, highlighting the need for cheap and synthetically accessible alternatives.[78]

Non-covalent interaction motifs, such as those based on hydrogen bonding groups, can also be scaffolded on amphiphilic monomers. The Meijer group has investigated four-fold hydrogen-bond providing ureidopyrimidinone (UPy) units on several biomedically relevant polymers such as polycaprolactone (PCL),[89] oligo[90] (OEG) and poly(ethylene glycol) (PEG).[91] On amphiphilic scaffolds, UPy-based monomers self-assemble into fibers through hydrophobic, hydrogen bonding and π-π interactions, to form injectable and self-healable supramolecular hydrogel materials for engineering kidney and cardiac tissues (Figure 1.8B).[92,93] Similarly, structures based on benzene-1,3,5-tricarboxamides (BTA) with ethylene glycol modification have been designed to fabricate supramolecular polymers in water through hydrogen bonding, hydrophobic and π-π interactions from the benzene moiety.[94–97] The dynamic properties of the BTA-based supramolecular polymers was demonstrated via Forster resonance energy transfer (FRET),[98] stochastic optical reconstruction microscopy (STORM)[99] and hydrogen/deuterium exchange (HDX) mass spectrometry,[100] respectively. These monomers have shown promise as supramolecular polymer nanoparticles for the intracellular delivery of siRNA and cargo molecules.

More recently, we have validated the use of squaramides to engineer supramolecular biomaterials. Self-assembly of bis-squaramide bolaamphiphiles in water resulted in micrometer-long supramolecular fibers that were visualized by cryogenic transmission electron microscopy (cryo-TEM) and small angle X-ray scattering (SAXS) with a uniform diameter (Figure 1.8C). The hydrogen bonding of the bis-squaramides in a head-to-tail arrangement enhanced the aromatic character of the squaramide ring as evidenced by computational studies, increasing thermodynamic stability of the whole self-assembled structure.[101] By modulating the peripheral PEG and aliphatic chain lengths of the squaramide-based bolaamphiphiles, a morphological

transition from fibres to spheres was observed and a tunable biodistribution behavior *in vivo*.[102] Fibrous structures displayed short blood circulation and rapid capture by venous endothelial cells, whereas spherical aggregates showed significantly longer blood circulation and less accumulation in the caudal vein within the zebrafish embryo model.[103] Furthermore, we reported a novel tripodal tris(2-aminoethyl)amine core (TREN)-based squaramide monomer, in which three squaramide units are embedded within a flexible hydrophobic core (Figure 1.8D). Monomer aggregation was mainly driven by hydrophobic forces and hydrogen bonding of the squaramide moieties, leading to a hydrogel network of entangled micrometer fibrils. These supramolecular hydrogels show self-recovering behavior and are validated to support 3D culture of hiPSCs and their derivatives (Figure 1.8D).[104] While, the lack of bioactive units in this TREN-based hydrogel limit their further applications in this area, such as introducing cell adhesion peptides to engineer cell-matrix interactions for cell culture *in vitro*.

Figure 1.8. A) PAs monomer structure and self-assembly into cylindrical high aspect ratio nanofibers under physiological conditions. Image adapted from reference [83]. B)

Upy-based monomers (with or without functional groups) co-assemble into fibers through directional hydrophobic and hydrogen bonding interactions. Image adapted from reference [105]. C) Squaramide-based bolaamphiphiles chemical structure and intermolecular stacking through directional hydrogen bonding interactions. Image adapted from reference [101]. D) TREN-based squaramide monomer chemical structure and its self-assembly into supramolecular hydrogels. Image adapted from reference [104].

With a better understanding of supramolecular self-assembly principles, researchers are able to design novel functional polymers through a modular co-assembly approach that combines functional monomers together with their native counterparts. The functional groups can be either embedded within the central core of the monomer or tethered on the periphery in a defined manner through chemical synthesis. Stupp and co-workers have incorporated the functional peptide IKVAV that is derived from laminin and known to promote neurite formation, into the PA backbone obtaining a scaffold that rapidly induces neural lineage differentiation from neural progenitor cells.[106] Similarly, VEGF mimicking sequences were incorporated in PA backbone resulting in nanoscale filaments that present VEGF-mimetic peptides with a high density to activate VEGF receptors and promote angiogenesis in endothelial cells displaying enhanced cell proliferation activity, viability, migration and angiogenic response.[107] One of the attractive aspects of the co-assembly approach is its modularity, i.e. it enables the facile formation of functional polymers through the co-assembly of different monomers through mixing and matching. For example, an RGDS-presenting PA co-assembled together with the native PA results in an RGD-functionalized PA scaffold. Bone marrow-derived stem cells and progenitor cells encapsulated within this bioactive scaffold were observed to show enhanced cell attachment, cell proliferation and expression of endothelial-specific markers due to the presentation of this cell adhesive motif.[108] Another notable example of co-assembly is

reported by Albertazzi *et al.*, in which a BTA monomer that is positively charged and fluorescently-labelled co-assembles into functional supramolecular polymers that encapsulate Nile Red and electrostatically bind siRNA showing the facile nature of this approach to fabricate supramolecular nanoparticles with dual delivery function.[109]

Overall, supramolecular polymers show great potential to mimic the native ECM with respect to their reversibility, dynamic character and fibrous structure. Moreover, their modularity in the introduction of bioactive motifs is especially attractive for engineering *in vivo* microenvironment for 3D cell culture and tissue engineering applications, and more broadly, in healthcare.

1.7 Aim and outline

In this thesis, I focus on the preparation of fully synthetic and functional dynamic polymer biomaterials and investigate their application as scaffolds for 3D cell culture *in vitro*, including cancer cell spheroids, hiPSC expansion and differentiation to cardiomyocytes, enhancing maturity of hESCs-derived cardiomyocytes and supporting primary chondrocytes with matrix production.

In **Chapter 2**, I develop a bioactive supramolecular polymer hydrogel through a co-assembly approach. Next to the native squaramide-based monomers, a novel azide-functionalized squaramide-based monomer was prepared to introduce short bioactive peptides. The co-assembly process is characterized by UV-vis spectroscopy, Cryo-TEM, and the hydrogel mechanical properties will be investigated by oscillatory rheology. HepG2 cells are encapsulated within this bioactive hydrogel to understand their potential to support their metabolic maturation.

In **Chapter 3**, I examine the potential for multicomponent supramolecular self-assembly through the introduction of two integrin-targeting peptides for human induced pluripotent stem cell expansion. The co-assembly process is characterized by UV-vis spectroscopy, Cryo-TEM, and the hydrogel mechanical properties will be

investigated by oscillatory rheology. Two hiPSCs cell lines are be encapsulated within these supramolecular hydrogels for 4 days, and in some cases for 3 passages. After expansion, the cell viability, proliferation, pluripotent marker expression, differentiation potential and genetic stability of hiPSCs will be evaluated.

In **Chapter 4**, I introduce a disulfide-based dynamic covalent crosslink in a covalent PEG hydrogel system using a cyclic thiosulfinate. Together with a static covalent crosslink based on thiol Michael addition, we make a dual-crosslinked and dynamic PEG hydrogel. This dynamic PEG hydrogel is investigated with respect to its mechanical and swelling properties, and cytocompatibility. The hESC-derived cardiomyocytes are encapsulated within both static and dynamic PEG hydrogels to evaluate the impact of dynamics on cardiomyocyte behavior.

In **Chapter 5**, I employ an the inverse electron-demand Diels–Alder (iEDDA) reaction to prepare covalent PEG hydrogels using the gas evolution from the bioconjugation reaction to result in pores with diameters on the order of hundred micrometers. The mechanical properties and pore formation are evaluated by oscillatory rheology and confocal microscopy. Primary chondrocytes are cultured within the porous hydrogel, and their viability and subsequently, cell matrix production is investigated.

Chapter 6 summarizes all the synthetic designs and experimental results presented in this thesis. Conclusions and some future prospect are included.

1.7 References

[1]   R. K. Harrison, *Nat. Rev. Drug Discov.* **2016**, *15*, 817.

[2]   A. L. Howes, R. D. Richardson, D. Finlay, K. Vuori, *PLoS One* **2014**, *9*.

[3]   S. Cassim, V. A. Raymond, P. Lapierre, M. Bilodeau, *PLoS One* **2017**, *12*, 1.

[4]   S. Sant, P. A. Johnston, *Drug Discov. Today Technol.* **2017**, *23*, 27.

[5]   W. Liao, J. Wang, J. Xu, F. You, M. Pan, X. Xu, J. Weng, X. Han, S. Li, Y. Li, K. Liang, Q. Peng, Y. Gao, *J. Tissue Eng.* **2019**, *10*.

[6]   D. S. Reynolds, K. M. Tevis, W. A. Blessing, Y. L. Colson, M. H. Zaman, M. W. Grinstaff, *Sci. Rep.* **2017**, *7*, 1.

[7]   A. Daly, M. Davidson, J. Burdick, *Nat. Commun.* **2021**, *12*, 753.

[8]   M. Vinci, S. Gowan, F. Boxall, L. Patterson, M. Zimmermann, W. Court, C. Lomas, M. Mendiola, D. Hardisson, S. A. Eccles, *BMC Biol.* **2012**, *10*, 29.

[9]   Z. Hannoun, C. Steichen, N. Dianat, A. Weber, A. Dubart-Kupperschmitt, *J. Hepatol.* **2016**, *65*, 182.

[10]   S. A. Langhans, *Front. Pharmacol.* **2018**, *9*, 1.

[11]   K. Takahashi, S. Yamanaka, *Cell* **2006**, *126*, 663.

[12]   K. Takahashi, K. Tanabe, M. Ohnuki, M. Narita, T. Ichisaka, K. Tomoda, S. Yamanaka, *Cell* **2007**, *131*, 861.

[13]   J. Zhang, G. F. Wilson, A. G. Soerens, C. H. Koonce, J. Yu, S. P. Palecek, J. A. Thomson, T. J. Kamp, *Circ. Res.* **2009**, *104*, 30.

[14]   S. Conrad, M. Renninger, J. Hennenlotter, T. Wiesner, L. Just, M. Bonin, W. Aicher, H. J. Bühring, U. Mattheus, A. Mack, H. J. Wagner, S. Minger, M. Matzkies, M. Reppel, J. Hescheler, K. D. Sievert, A. Stenzl, T. Skutella, *Nature* **2008**, *456*, 344.

[15]   T. Aasen, A. Raya, M. J. Barrero, E. Garreta, A. Consiglio, F. Gonzalez, R. Vassena, J. Bilić, V. Pekarik, G. Tiscornia, M. Edel, S. Boué, J. C. I. Belmonte, *Nat. Biotechnol.* **2008**, *26*, 1276.

[16]   K. Okita, Y. Matsumura, Y. Sato, A. Okada, A. Morizane, S. Okamoto, H. Hong, M. Nakagawa, K. Tanabe, K. I. Tezuka, T. Shibata, T. Kunisada, M. Takahashi, J. Takahashi, H. Saji, S. Yamanaka, *Nat. Methods* **2011**, *8*, 409.

[17]   K. Kaji, K. Norrby, A. Paca, M. Mileikovsky, P. Mohseni, K. Woltjen, *Nature* **2009**, *458*, 771.

[18]   D. Huangfu, K. Osafune, R. Maehr, W. Guo, A. Eijkelenboom, S. Chen, W. Muhlestein, D. A. Melton, *Nat. Biotechnol.* **2008**, *26*, 1269.

[19]   A. Wang, Z. Tang, I. H. Park, Y. Zhu, S. Patel, G. Q. Daley, S. Li, *Biomaterials* **2011**, *32*, 5023.

[20]   F. Bastami, P. Nazeman, H. Moslemi, M. Rezai Rad, K. Sharifi, A. Khojasteh, *Cell Prolif.* **2017**, *50*.

[21]   J. Jang, J. E. Yoo, J. A. Lee, D. R. Lee, J. Y. Kim, Y. J. Huh, D. S. Kim, C. Y. Park, D. Y. Hwang, H. S. Kim, H. C. Kang, D. W. Kim, *Exp. Mol. Med.* **2012**, *44*, 202.

[22]   Y. S. Chun, P. Chaudhari, Y. Y. Jang, *Int. J. Biol. Sci.* **2010**, *6*, 796.

[23]   A. S. T. Smith, J. Macadangdang, W. Leung, M. A. Laflamme, D. H. Kim, *Biotechnol. Adv.* **2017**, *35*, 77.

[24]   Y. Li, L. Li, Z. N. Chen, G. Gao, R. Yao, W. Sun, *Biofabrication* **2017**, *9*.

[25]   M. Richards, C. Y. Fong, W. K. Chan, P. C. Wong, A. Bongso, *Nat. Biotechnol.* **2002**, *20*, 933.

[26]   S. Jin, H. Yao, J. L. Weber, Z. K. Melkoumian, K. Ye, *PLoS One* **2012**, *7*.

[27]   Z. Melkoumian, J. L. Weber, D. M. Weber, A. G. Fadeev, Y. Zhou, P. Dolley-Sonneville, J. Yang, L. Qiu, C. A. Priest, C. Shogbon, A. W. Martin, J. Nelson, P. West, J. P. Beltzer, S. Pal, R. Brandenberger, *Nat. Biotechnol.* **2010**, *28*, 606.

[28]   J. R. Klim, L. Li, P. J. Wrighton, M. S. Piekarczyk, L. L. Kiessling, *Nat. Methods* **2010**, *7*, 989.

[29]   C. McKee, G. R. Chaudhry, *Colloids Surfaces B Biointerfaces* **2017**, *159*, 62.

[30]   R. Passier, V. Orlova, C. Mummery, *Cell Stem Cell* **2016**, *18*, 309.

[31]   E. Giacomelli, M. Bellin, V. V. Orlova, C. L. Mummery, *Curr. Protoc. Hum. Genet.* **2017**, *95*, 21.9.1.

[32]   D. T. Paik, M. Chandy, J. C. Wu, *Pharmacol. Rev.* **2020**, *72*, 320.

[33]   S. Funakoshi, K. Miki, T. Takaki, C. Okubo, T. Hatani, K. Chonabayashi, M. Nishikawa, I. Takei, A. Oishi, M. Narita, M. Hoshijima, T. Kimura, S. Yamanaka, Y. Yoshida, *Sci. Rep.* **2016**, *6*, 1.

[34]   X. Guan, W. Xu, H. Zhang, Q. Wang, J. Yu, R. Zhang, Y. Chen, Y. Xia, J. Wang, D. Wang, *Stem Cell Res. Ther.* **2020**, *11*, 1.

[35]   Y. Luo, C. Lou, S. Zhang, Z. Zhu, Q. Xing, P. Wang, T. Liu, H. Liu, C. Li, W. Shi, Z. Du, Y. Gao, *Cytotherapy* **2018**, *20*, 95.

[36]   C. Frantz, K. M. Stewart, V. M. Weaver, *J. Cell Sci.* **2010**, *123*, 4195.

[37]   S. R. Braam, L. Zeinstra, S. Litjens, D. Ward-van Oostwaard, S. van den Brink, L.

van Laake, F. Lebrin, P. Kats, R. Hochstenbach, R. Passier, A. Sonnenberg, C. L. Mummery, *Stem Cells* **2008**, *26*, 2257.

[38]   S. Rodin, A. Domogatskaya, S. Ström, E. M. Hansson, K. R. Chien, J. Inzunza, O. Hovatta, K. Tryggvason, *Nat. Biotechnol.* **2010**, *28*, 611.

[39]   M. P. Lutolf, J. A. Hubbell, *Nat. Biotechnol.* **2005**, *23*, 47.

[40]   S. R. Braam, L. Zeinstra, S. Litjens, D. Ward-van Oostwaard, S. van den Brink, L. van Laake, F. Lebrin, P. Kats, R. Hochstenbach, R. Passier, A. Sonnenberg, C. L. Mummery, *Stem Cells* **2008**, *26*, 2257.

[41]   C. Bonnans, J. Chou, Z. Werb, *Nat. Rev. Mol. Cell Biol.* **2014**, *15*, 786.

[42]   F. Gattazzo, A. Urciuolo, P. Bonaldo, *Biochim. Biophys. Acta - Gen. Subj.* **2014**, *1840*, 2506.

[43]   J. L. Young, A. J. Engler, *Biomaterials* **2011**, *32*, 1002.

[44]   A. J. Engler, S. Sen, H. L. Sweeney, D. E. Discher, *Cell* **2006**, *126*, 677.

[45]   P. M. Gilbert, K. L. Havenstrite, K. E. G. Magnusson, A. Sacco, N. A. Leonardi, P. Kraft, N. K. Nguyen, S. Thrun, M. P. Lutolf, H. M. Blau, *Science (80).* **2010**, *329*, 1078.

[46]   P. C. Georges, W. J. Miller, D. F. Meaney, E. S. Sawyer, P. A. Janmey, *Biophys. J.* **2006**, *90*, 3012.

[47]   N. Huebsch, P. R. Arany, A. S. Mao, D. Shvartsman, O. A. Ali, S. A. Bencherif, J. Rivera-Feliciano, D. J. Mooney, *Nat. Mater.* **2010**, *9*, 518.

[48]   N. Huebsch, E. Lippens, K. Lee, M. Mehta, S. T. Koshy, M. C. Darnell, R. M. Desai, C. M. Madl, M. Xu, X. Zhao, O. Chaudhuri, C. Verbeke, W. S. Kim, K. Alim, A. Mammoto, D. E. Ingber, G. N. Duda, D. J. Mooney, *Nat. Mater.* **2015**, *14*, 1269.

[49]   F. Edalat, I. Sheu, S. Manoucheri, A. Khademhosseini, *Curr. Opin. Biotechnol.* **2012**, *23*, 820.

[50]   G. J. Pahapale, S. Gao, L. H. Romer, D. H. Gracias, *ACS Appl. Bio Mater.* **2019**, *2*, 6004.

[51]   H. Tekin, S. Simmons, B. Cummings, L. Gao, X. Adiconis, C. C. Hession, A. Ghoshal, D. Dionne, S. R. Choudhury, V. Yesilyurt, N. E. Sanjana, X. Shi, C. Lu, M. Heidenreich, J. Q. Pan, J. Z. Levin, F. Zhang, *Nat. Biomed. Eng.* **2018**, *2*, 540.

[52] G. Huang, F. Li, X. Zhao, Y. Ma, Y. Li, M. Lin, G. Jin, T. J. Lu, G. M. Genin, F. Xu, *Chem. Rev.* **2017**, *117*, 12764.

[53] E. S. Place, J. H. George, C. K. Williams, M. M. Stevens, *Chem. Soc. Rev.* **2009**, *38*, 1139.

[54] P. M. Kharkar, K. L. Kiick, A. M. Kloxin, *Chem. Soc. Rev.* **2013**, *42*, 7335.

[55] M. Parlato, S. Reichert, N. Barney, W. L. Murphy, *Macromol. Biosci.* **2014**, *14*, 687.

[56] T. E. Brown, J. S. Silver, B. T. Worrell, I. A. Marozas, F. M. Yavitt, K. A. Günay, C. N. Bowman, K. S. Anseth, *J. Am. Chem. Soc.* **2018**, *140*, 11585.

[57] J. Zhu, *Biomaterials* **2010**, *31*, 4639.

[58] K. A. Kyburz, K. S. Anseth, *Acta Biomater.* **2013**, *9*, 6381.

[59] E. M. Ovadia, D. W. Colby, A. M. Kloxin, *Biomater. Sci.* **2018**, *6*, 1358.

[60] S. Q. Liu, P. L. Rachel Ee, C. Y. Ke, J. L. Hedrick, Y. Y. Yang, *Biomaterials* **2009**, *30*, 1453.

[61] Z. Wei, R. Schnellmann, H. C. Pruitt, S. Gerecht, *Cell Stem Cell* **2020**, *27*, 798.

[62] S. Tang, H. Ma, H. C. Tu, H. R. Wang, P. C. Lin, K. S. Anseth, *Adv. Sci.* **2018**, *5*, 1.

[63] Y. Chen, D. Diaz-Dussan, D. Wu, W. Wang, Y. Y. Peng, A. B. Asha, D. G. Hall, K. Ishihara, R. Narain, *ACS Macro Lett.* **2018**, *7*, 904.

[64] S. Y. Choh, D. Cross, C. Wang, *Biomacromolecules* **2011**, *12*, 1126.

[65] F. Yang, J. Wang, L. Cao, R. Chen, L. Tang, C. Liu, *J. Mater. Chem. B* **2014**, *2*, 295.

[66] G. A. Barcan, X. Zhang, R. M. Waymouth, *J. Am. Chem. Soc.* **2015**, *137*, 5650.

[67] C. M. Madl, S. C. Heilshorn, *Chem. Mater.* **2019**, *31*, 8035.

[68] S. Mukherjee, M. R. Hill, B. S. Sumerlin, *Soft Matter* **2015**, *11*, 6152.

[69] M. D. Konieczynska, J. C. Villa-Camacho, C. Ghobril, M. Perez-Viloria, K. M. Tevis, W. A. Blessing, A. Nazarian, E. K. Rodriguez, M. W. Grinstaff, *Angew. Chemie* **2016**, *128*, 10138.

[70] T. E. Brown, B. J. Carberry, B. T. Worrell, O. Y. Dudaryeva, M. K. McBride, C. N. Bowman, K. S. Anseth, *Biomaterials* **2018**, *178*, 496.

[71] Z. Wei, D. M. Lewis, Y. Xu, S. Gerecht, *Adv. Healthc. Mater.* **2017**, *6*, 1.

[72] Z. Wei, S. Gerecht, *Biomaterials* **2018**, *185*, 86.

[73] D. D. McKinnon, D. W. Domaille, J. N. Cha, K. S. Anseth, *Adv. Mater.* **2014**, *26*, 865.

[74] P. K. Sharma, S. Taneja, Y. Singh, *ACS Appl. Mater. Interfaces* **2018**, *10*, 30936.

[75] Z. Li, F. Zhou, Z. Li, S. Lin, L. Chen, L. Liu, Y. Chen, *ACS Appl. Mater. Interfaces* **2018**, *10*, 25194.

[76] L. L. Wang, C. B. Highley, Y. C. Yeh, J. H. Galarraga, S. Uman, J. A. Burdick, *J. Biomed. Mater. Res. Part A* **2018**, *106*, 865.

[77] N. Gjorevski, N. Sachs, A. Manfrin, S. Giger, M. E. Bragina, P. Ordóñez-Morán, H. Clevers, M. P. Lutolf, *Nature* **2016**, *539*, 560.

[78] M. J. Webber, E. A. Appel, E. W. Meijer, R. Langer, *Nat. Mater.* **2015**, *15*, 13.

[79] R. G. Ellis-Behnke, Y. X. Liang, S. W. You, D. K. C. Tay, S. Zhang, K. F. So, G. E. Schneider, *Proc. Natl. Acad. Sci. U. S. A.* **2006**, *103*, 5054.

[80] S. Zhang, *Second Smith Nephew Int. Symp. - Tissue Eng. 2000 Adv. Tissue Eng. Biomater. Cell Signal.* **2000**, 12.

[81] N. L. Francis, N. K. Bennett, A. Halikere, Z. P. Pang, P. V. Moghe, *ACS Biomater. Sci. Eng.* **2016**, *2*, 1030.

[82] W. Shi, C. J. Huang, X. D. Xu, G. H. Jin, R. Q. Huang, J. F. Huang, Y. N. Chen, S. Q. Ju, Y. Wang, Y. W. Shi, J. B. Qin, Y. Q. Zhang, Q. Q. Liu, X. B. Wang, X. H. Zhang, J. Chen, *Acta Biomater.* **2016**, *45*, 247.

[83] T. J. Mitchison, J. C. Biol, J. F. Kelleher, S. J. Atkinson, T. D. Pollard, J. C. Biol, J. D. Hartgerink, E. Beniash, S. I. Stupp, **2001**, *294*, 1684.

[84] J. D. Hartgerink, E. Beniash, S. I. Stupp, *Proc. Natl. Acad. Sci. U. S. A.* **2002**, *99*, 5133.

[85] H. Cui, T. Muraoka, A. G. Cheetham, S. I. Stupp, *Nano Lett.* **2009**, *9*, 945.

[86] R. N. Shah, N. A. Shah, M. M. D. R. Lim, C. Hsieh, G. Nuber, S. I. Stupp, *Proc. Natl. Acad. Sci. U. S. A.* **2010**, *107*, 3293.

[87] R. S. Tu, R. Marullo, R. Pynn, R. Bitton, H. Bianco-Peled, M. V. Tirrell, *Soft Matter* **2010**, *6*, 1035.

[88] K. Rajangam, H. A. Behanna, M. J. Hui, X. Han, J. F. Hulvat, J. W. Lomasney, S. I.

Stupp, *Nano Lett.* **2006**, *6*, 2086.

[89] P. Y. W. Dankers, E. N. M. van Leeuwen, G. M. L. van Gemert, A. J. H. Spiering, M. C. Harmsen, L. A. Brouwer, H. M. Janssen, A. W. Bosman, M. J. A. van Luyn, E. W. Meijer, *Biomaterials* **2006**, *27*, 5490.

[90] R. E. Kieltyka, M. M. C. Bastings, G. C. van Almen, P. Besenius, E. W. L. Kemps, P. Y. W. Dankers, *Chem. Commun.* **2012**, *48*, 1452.

[91] P. Y. W. Dankers, T. M. Hermans, T. W. Baughman, Y. Kamikawa, R. E. Kieltyka, M. M. C. Bastings, H. M. Janssen, N. A. J. M. Sommerdijk, A. Larsen, M. J. A. Van Luyn, A. W. Bosman, E. R. Popa, G. Fytas, E. W. Meijer, *Adv. Mater.* **2012**, *24*, 2703.

[92] P. Y. W. Dankers, M. J. A. Van Luyn, A. Huizinga-Van Der Vlag, A. H. Petersen, J. A. Koerts, A. W. Bosman, E. R. Popa, *Eur. Polym. J.* **2015**, *72*, 484.

[93] M. M. C. Bastings, S. Koudstaal, R. E. Kieltyka, Y. Nakano, A. C. H. Pape, D. A. M. Feyen, F. J. van Slochteren, P. A. Doevendans, J. P. G. Sluijter, E. W. Meijer, S. A. J. Chamuleau, P. Y. W. Dankers, *Adv. Healthc. Mater.* **2014**, *3*, 70.

[94] P. J. M. Stals, M. M. J. Smulders, R. Martín-Rapún, A. R. A. Palmans, E. W. Meijer, *Chem. - A Eur. J.* **2009**, *15*, 2071.

[95] M. M. J. Smulders, I. A. W. Filot, J. M. A. Leenders, P. Van Der Schoot, A. R. A. Palmans, A. P. H. J. Schenning, E. W. Meijer, *J. Am. Chem. Soc.* **2010**, *132*, 611.

[96] S. Cantekin, T. F. A. de Greef, A. R. A. Palmans, *Chem. Soc. Rev.* **2012**, *41*, 6125.

[97] F. Paquin, J. Rivnay, A. Salleo, N. Stingelin, C. Silva, *J. Mater. Chem. C* **2015**, *3*, 10715.

[98] L. Albertazzi, F. J. Martinez-Veracoechea, C. M. A. Leenders, I. K. Voets, D. Frenkel, E. W. Meijer, *Proc. Natl. Acad. Sci. U. S. A.* **2013**, *110*, 12203.

[99] L. Albertazzi, D. Van Der Zwaag, C. M. A. Leenders, R. Fitzner, R. W. Van Der Hofstad, E. W. Meijer, *Science (80).* **2014**, *344*, 491.

[100] X. Lou, R. P. M. Lafleur, C. M. A. Leenders, S. M. C. Schoenmakers, N. M. Matsumoto, M. B. Baker, J. L. J. Van Dongen, A. R. A. Palmans, E. W. Meijer, *Nat. Commun.* **2017**, *8*, 1.

[101] V. Saez Talens, P. Englebienne, T. T. Trinh, W. E. M. Noteborn, I. K. Voets, R. E. Kieltyka, *Angew. Chemie* **2015**, *127*, 10648.

[102] V. Saez Talens, D. M. M. Makurat, T. Liu, W. Dai, C. Guibert, W. E. M. Noteborn, I. K. Voets, R. E. Kieltyka, *Polym. Chem.* **2019**, *10*, 3146.

[103] V. Saez Talens, G. Arias-Alpizar, D. M. M. Makurat, J. Davis, J. Bussmann, A. Kros, R. E. Kieltyka, *Biomacromolecules* **2020**, *21*, 1060.

[104] C. Tong, T. Liu, V. Saez Talens, W. E. M. Noteborn, T. H. Sharp, M. M. R. M. Hendrix, I. K. Voets, C. L. Mummery, V. V. Orlova, R. E. Kieltyka, *Biomacromolecules* **2018**, *19*, 1091.

[105] S. I. S. Hendrikse, S. P. W. Wijnands, R. P. M. Lafleur, M. J. Pouderoijen, H. M. Janssen, P. Y. W. Dankers, E. W. Meijer, *Chem. Commun.* **2017**, *53*, 2279.

[106] G. A. Silva, C. Czeisler, K. L. Niece, E. Beniash, D. A. Harrington, J. A. Kessler, S. I. Stupp, *Science (80).* **2004**, *303*, 1352.

[107] M. J. Webber, J. Tongers, C. J. Newcomb, K. T. Marquardt, J. Bauersachs, D. W. Losordo, S. I. Stupp, *Proc. Natl. Acad. Sci. U. S. A.* **2012**, *109*, 9220.

[108] M. J. Webber, J. Tongers, M. A. Renault, J. G. Roncalli, D. W. Losordo, S. I. Stupp, *Acta Biomater.* **2010**, *6*, 3.

[109] M. H. Bakker, C. C. Lee, E. W. Meijer, P. Y. W. Dankers, L. Albertazzi, *ACS Nano* **2016**, *10*, 1845.